ARTICLE

A three-dimensional *ex vivo* tri-culture model mimics cell-cell interactions between acute myeloid leukemia and the vascular niche

Laura J. Bray,[1,2] Marcus Binner,[1] Yvonne Körner,[1] Malte von Bonin,[3-5] Martin Bornhäuser[3-5] and Carsten Werner[1]

[1]Max Bergmann Center of Biomaterials, Leibniz Institute of Polymer Research Dresden, Germany; [2]Science and Engineering Faculty, Queensland University of Technology, Brisbane, Australia; [3]Universitätsklinikum Carl-Gustav Carus, Faculty of Medicine, Technische Universität Dresden, Saxony, Germany; [4]German Cancer Center (DKFZ), Heidelberg, Germany and [5]German Cancer Consortium (DKTK), partner site Dresden, Germany

Haematologica 2017
Volume 102(7):1215-1226

ABSTRACT

Ex vivo studies of human disease, such as acute myeloid leukemia, are generally limited to the analysis of two-dimensional cultures which often misinterpret the effectiveness of chemotherapeutics and other treatments. Here we show that matrix metalloproteinase-sensitive hydrogels prepared from poly(ethylene glycol) and heparin functionalized with adhesion ligands and pro-angiogenic factors can be instrumental to produce robust three-dimensional culture models, allowing for the analysis of acute myeloid leukemia development and response to treatment. We evaluated the growth of four leukemia cell lines, KG1a, MOLM13, MV4-11 and OCI-AML3, as well as samples from patients with acute myeloid leukemia. Furthermore, endothelial cells and mesenchymal stromal cells were co-seeded to mimic the vascular niche for acute myeloid leukemia cells. Greater drug resistance to daunorubicin and cytarabine was demonstrated in three-dimensional cultures and in vascular co-cultures when compared with two-dimensional suspension cultures, opening the way for drug combination studies. Application of the C-X-C chemokine receptor type 4 (CXCR4) inhibitor, AMD3100, induced mobilization of the acute myeloid leukemia cells from the vascular networks. These findings indicate that the three-dimensional tri-culture model provides a specialized platform for the investigation of cell-cell interactions, addressing a key challenge of current testing models. This *ex vivo* system allows for personalized analysis of the responses of patients' cells, providing new insights into the development of acute myeloid leukemia and therapies for this disease.

Correspondence:
Laura.bray@qut.edu.au

Received: October 8, 2016
Accepted: March 27, 2017
Pre-published: March 30, 2017.

doi:10.3324/haematol.2016.157883

Check the online version for the most updated information on this article, online supplements, and information on authorship & disclosures: www.haematologica.org/content/102/7/1215

Introduction

At the interface of *in vitro* culture models and complex animal models are sophisticated *ex vivo* models, which rely on our ability to replicate tissue microenvironments in order to sustain the growth of donor cells. Cell-cell and cell-matrix interactions, together with the signaling mechanisms between cells residing within spatially distinct niches, are important for the analysis of disease development and progression, and responses to drugs. Acute myeloid leukemia (AML) is a disease associated with 5-year survival rates of less than 40% in adults,[1-3] although this figure decreases to less than 10% for adults aged over 65 years old.[2,3] AML is characterized by an uncontrolled expansion of immature blasts resulting in a reduced normal blood cell production. Leukemic cell proliferation and resistance to chemotherapy have remained difficult to investigate *ex vivo*[4,5] since conventional two-dimensional (2D) cell cultures cannot provide long-term maintenance of primary leukemic cells

without the support of additional growth factors or stromal cells and lack the microenvironmental stimuli of the bone marrow.

Different bioengineered three-dimensional (3D) culture systems have, therefore, been developed to study AML cells *in vitro* more realistically using, however, stiff and porous materials as scaffolds and mono-cultures or co-cultures of AML with mesenchymal stromal cells (MSC).[6-8] While these systems replicated important aspects of the stromal microenvironment, they did not allow for the exploration of leukemic-vascular cell-cell interactions which are critical for leukemia biology and progression.[9] The vascular niche, so-called due to its density of blood vessels, is a location where endothelial cells and mural cells, such as pericytes, generate a microenvironment that influences the behavior of hematopoietic and leukemic stem and progenitor cells.[10] In particular, angiogenesis is promoted by the bone marrow stroma and leukemic blasts and further increases in conditions such as AML and acute lymphoblastic leukemia.[11-13] Activation by angiogenic growth factors and cytokines, such as vascular endothelial growth factor, stromal cell-derived factor 1 and fibroblast growth factor 2, modify the vascular niche to promote malignant growth.[14] While a relationship between AML and vascular endothelium seems likely to contribute to the progression of AML, the mechanisms involved in these interactions are not yet understood.[15-17]

To recapitulate AML-vascular niche interactions *in vitro*, we used a set of thoroughly defined and widely tunable star-shaped poly(ethylene glycol) (starPEG)-heparin hydrogels[18,19] to grow cells from four leukemia lines, KG1a, MOLM13, MV4-11 and OCI-AML3, as well as primary cells from AML patients, with human vascular endothelial cells as well as MSC. To support the specific requirements of the chosen cell types, the gel matrices were functionalized with precisely adjusted amounts of covalently attached adhesion receptor ligand peptide (RGD) motifs. Matrix metalloproteinase-responsive peptide sequences were incorporated as hydrogel crosslinkers to allow for localized cellular remodeling, thus supporting proliferation and migration of cells within the 3D gel cultures. A combination of growth factors (vascular endothelial growth factor, fibroblast growth factor 2, stromal cell-derived factor 1) known to associate tightly with the glycosaminoglycan heparin was applied to customize the gel matrices according to previously established protocols to afford sustainable administration resulting in the formation and maintenance of 3D endothelial cell capillary networks within the gels.[20] To validate the culture model, we determined the impact of chemotherapeutics and signaling inhibitors on the tri-culture system and assessed the relevance of our findings. We applied a multi-disciplinary *in vitro* approach that integrates biological and physical techniques with human samples, ultimately extending our understanding of the impact of treatments on cell-cell interactions.

Methods

Culture of cell lines

KG1a, MOLM13, MV4-11 and OCI-AML3 cell lines were obtained from the *Deutsche Sammlung von Mikroorganismen und Zellkulturen* (DSMZ; Braunschweig, Germany) and used within 15 passages. KG1a, MOLM13 and MV4-11 cells were cultured in medium consisting of Roswell Park Memorial Institute (RPMI, Life Technologies, Darmstadt, Germany) medium supplemented with GlutaMax (Life Technologies), 10% fetal bovine serum (FBS; Hyclone Thermo Scientific, Schwerte, Germany) and 1% penicillin/streptomycin solution (PS; Life Technologies). OCI-AML3 cells were cultured in Dulbecco modified Eagle medium (DMEM, Life Technologies) supplemented with 10% FBS and 1% PS.

Culture of primary donor cells

The studies were approved by the institutional review boards of all participating centers of the Study Alliance Leukemia in agreement with the Declaration of Helsinki and registered with National Clinical Trial numbers 00180115 (AML96 trial), 00180102 (AML2003 trial) and 00180167 (AML60+ trial). Written informed consent had been obtained from each patient. Three peripheral blood samples derived from patients with AML were obtained with ethical permission from the Uniklinikum Dresden, prepared as previously described,[21] frozen, and thawed directly for experiments in hydrogels. Primary AML cells were cultured in medium consisting of StemSpan SFEM (Stem Cell Technologies, Grenoble, France) supplemented with 2% FBS for human myeloid long-term culture (Stem Cell Technologies), 1% L-glutamine, 1% PS solution (both from Life Technologies), 10 ng/mL FLT3L, 10 ng/mL stem cell factor, 10 ng/mL thrombopoietin, and 10 μg/mL interleukin 3 (all from R&D Systems, Minneapolis, USA). OCI-AML3 cells were cultured in DMEM supplemented with 10% FBS and 1% PS. Human umbilical vein endothelial cells (HUVEC) were isolated as previously described[22] and cultured in endothelial cell growth medium (Promocell, Heidelberg, Germany). MSC were derived from healthy volunteer donors after informed consent. The use of surplus bone marrow cells for MSC generation was approved by the ethics committee of the Technical University Dresden (Ethics approval ID: EK127042009). Bone marrow-derived MSC were isolated as previously described[23] and cultured in DMEM supplemented with 10% FBS and 1% PS. HUVEC and MSC were utilized for experiments between passages 1 - 6.

Statistics

All statistical analyses were performed using GraphPad Prism version 6. Data were analyzed using either one-way or two-way analysis of variance (ANOVA) (depending on the experiment) with post-hoc Tukey multiple comparisons' tests. Levels of statistical significance are reported (*P<0.05, **P<0.01, ***P<0.001 or ****P<0.0001).

Results

Acute myeloid leukemia-vascular interactions within starPEG-heparin hydrogels

A tri-culture model of AML-vascular interactions was established utilizing hydrogels of approximately 200-300 Pa stiffness (storage modulus) (Figure 1A), as this stiffness was reported optimal for the development of a robust endothelial network,[20] and preliminary data showed that the endothelial cells would not form vascular networks in γ1.0 (1500 Pa) hydrogels (*data not shown*). Hydrogels were stable after casting and easily transferred into medium (Figure 1B). All AML cell lines, KG1a, MOLM13, MV4-11 and OCI-AML3, grew similarly within the 3D model. The colonization and proliferation of AML cells was visualized via light microscopy (Figure 1C) and confocal microscopy (Figure 1D-H) after 1 week of tri-culture. AML cell lines predominantly grew along the HUVEC-MSC vascular net-

work. The AML cell lines were determined to proliferate in AML-HUVEC and AML-MSC co-cultures in a similar way as in the AML-HUVEC-MSC tri-cultures (Figure 2). AML cell proliferation resulted in a heterogeneous mixture of spheroids and loose cell clumps in contact with the vascular network (Figure 1E,F). Primary donor cells from patients with leukemia (pAML) grew more slowly than the AML cell lines, resulting in less dense areas of AML-vascular interactions (Figure 1I-K). However, pAML cells appeared as clumps within the vascular network branching (Figure 1I), rarely formed spheroids, and showed preference for single cell adherence and growth to the HUVEC-MSC network (Figure 1J,K). The HUVEC-MSC population displayed expression of CD31, M-CAM, αSMA, and CD90 (*Online Supplementary Figure S1*).

Acute myeloid leukemia cells form spheroids within starPEG-heparin hydrogels

AML mono-culture models were generated by culturing KG1a, MOLM13, MV4-11 and OCI-AML3 cells within starPEG-heparin hydrogels of various stiffness or in Matrigel™ over 2 weeks. To determine the optimal stiff-

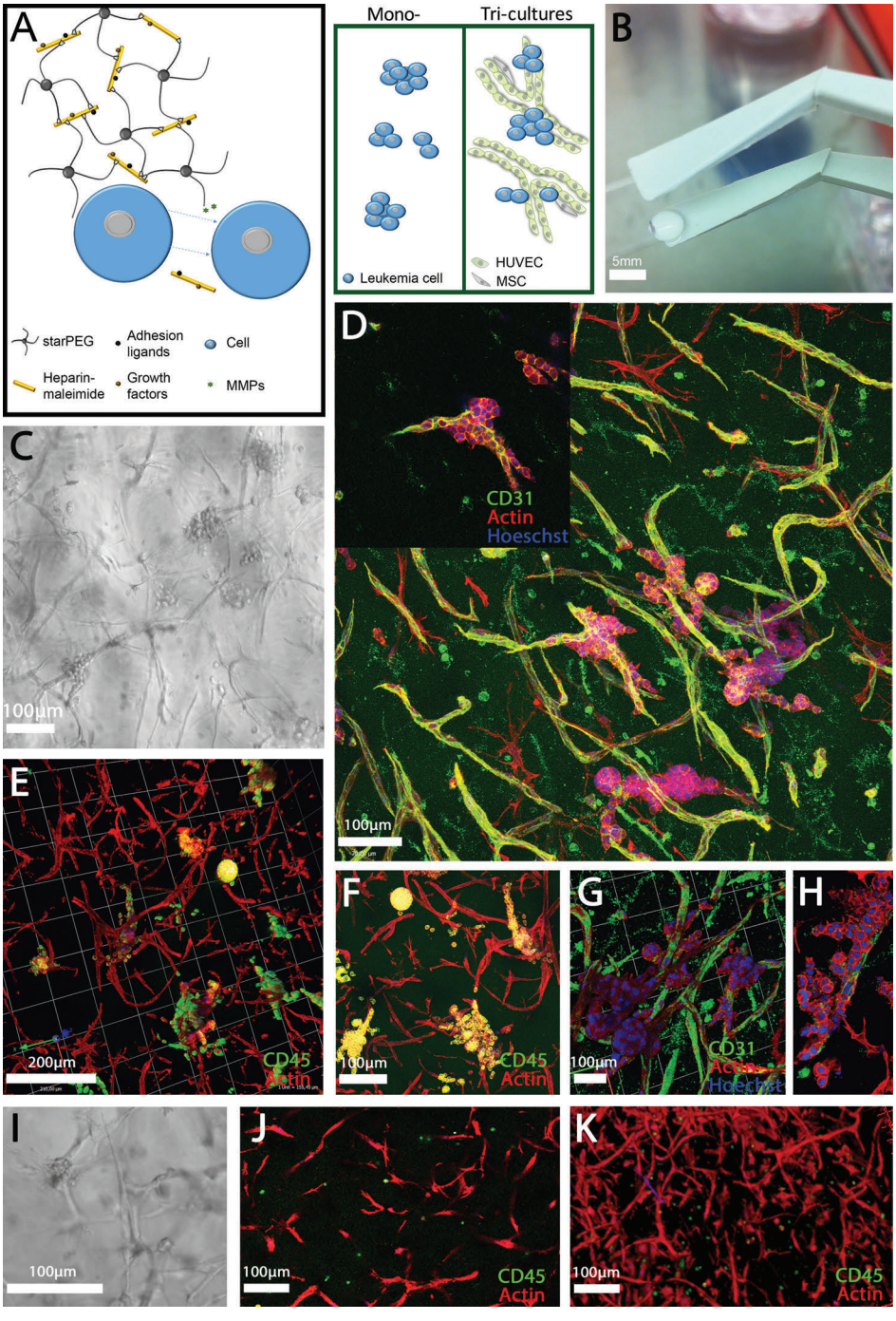

Figure 1. A three-dimensional culture model of acute myeloid leukemia-vascular interactions. (A) A biohybrid starPEG-heparin hydrogel was utilized which allows for the culture of AML mono-cultures and tri-cultures with HUVEC and bone marrow-derived MSC. B) Macroscopic image of final cast hydrogel before culture. Scale bar = 5 mm. (C) Light microscope and (D,H) confocal images of the OCI-AML3 cell line (as a representative of all cell lines utilized in this study) in tri-culture with HUVEC and MSC after 7 days depicting (D, G, H) CD31 and (E, F) CD45 expression. Images display leukemia cell growth primarily along the vascular endothelial cells. (I) Light microscope and confocal images (J,K) of primary donor cells from a patient with AML in tri-culture with HUVEC and MSC after 7 days. Scale bar = 100 and 200 µm as indicated. Images display the preference of leukemia cells to attach to and grow along vascular structures or within vascular branching.

ness for the culture of AML cells within starPEG-heparin hydrogels, three different cross-linking degrees were investigated (γ0.75, γ1, and γ1.5, where γ is the molar ratio of PEG to heparin). As previously described, the approximate stiffness of these cross-linking degrees equate to 500 Pa, 1500 Pa, and 3000 Pa (storage modulus), respectively.[24] Hydrogels prepared at γ0.75 often disintegrated during the culture period. Proliferation was measured using PrestoBlue reagent. Hydrogels prepared at γ1 allowed the greatest proliferation when compared with 2D cultures and contained spheroids of the largest size amongst all cross-linking degrees (Figure 3A-D). Matrigel™ cultures consistently allowed the greatest proliferation compared with both 2D cultures and starPEG-heparin cultures. Human pAML cells derived from three different donors were only cultured in γ1 hydrogels. In all three donor samples, a heterogeneous population of cells was present, as evidenced by the mixture of spheroids, loose cell clumps, and single cells (Figure 3E). In some cases, elongated cells were also present.

Acute myeloid leukemia cells display similar functionality and phenotype between two- and three-dimensional cultures

Migration assays and colony-forming assays were performed to determine whether the different matrices affected AML migratory abilities and clonogenicity, respectively. Migration of AML cells cultured in starPEG-heparin hydrogels was decreased compared to that in 2D cultures (*Online Supplementary Figure S2A*; KG1a: 67.51% ± 32.66; MOLM13: 66.93% ± 38.17; MV4-11: 29.82% ± 15.95; OCI-AML3: 38.27% ± 23.97). This might be due to residual hydrogel fragments blocking the pores. In the colony-forming experiment, while the number of MV4-11 colonies derived from 3D cultures was decreased compared with that from 2D cultures (55.45% ± 17.65), KG1a, MOLM13 and OCI-AML3 colony formation was not or only marginally reduced in 3D cultures (*Online Supplementary Figure S2B,C*; 87.08% ± 2.103; 98.06% ± 0.02; 88.16% ± 42.73). Flow cytometry analysis of 3D and 2D mono-cultures showed similar marker expression with the following exceptions. MOLM13 3D mono-cultures displayed higher mean fluorescence intensities (MFI) of CD33 and CD54, while MOLM13 2D cultures displayed higher MFI of CD29 (*Online Supplementary Figure S3A*). MV4-11 2D cultures showed higher MFI of HLA-DR and CD29 compared with 3D cultures. OCI-AML3 2D cultures demonstrated higher MFI of CD45 and CD54 than 3D cultures. Positive expression of target antigens in AML 3D and 2D cultures is detailed in *Online Supplementary Table S1*. Immunostaining for integrin α4, CD44 and CD54 was similar between all AML cells (*Online Supplementary Figure S3B*). Higher MFI of CD45 and HLA-DR was found in mono-cultures and higher MFI of CD49e and CD29 was found in pAML tri-cultures compared to mono-cultures. Immunostaining revealed similar expression of CD44 and CD34 in all three donors (*Online Supplementary Figure S3C*).

Acute myeloid leukemia three-dimensional tri-cultures demonstrate increased resistance to daunorubicin and cytarabine

The AML γ0.63 tri-cultures and γ1 mono-cultures were treated with seven different doses of daunorubicin and cytosine β-D-arabinofuranoside (cytarabine, AraC) and compared with 2D mono-cultures for 24 h. Compared with the 3D mono-cultures and tri-cultures, AML cells cultured in 2D were most sensitive to the drug doses applied (Figure 4B). Significant differences were found between KG1a 2D and 3D tri-culture cell viability after treatment with 0.20 μM daunorubicin (Figure 4B), and at all cytarabine concentrations tested except for 1,000 μM (*Online Supplementary Figure S4B*). MOLM13 tri-cultures were significantly more resistant than 2D cultures when treated with 0.10, 0.20 or 1.00 μM of daunorubicin (Figure 4B), and at most cytarabine concentrations (*Online Supplementary Figure S4B*). The number of viable cells was significantly higher in MV4-11 3D tri-cultures than 2D mono-cultures when treated with 0.01, 0.10, 0.20, 1.00, or 5.00 μM daunorubicin (Figure 4B), and at all cytarabine doses tested (*Online Supplementary Figure S4B*). Compared with 2D mono-cultures, OCI-AML3 3D tri-cultures displayed higher numbers of viable cells at 0.10 and 0.20 μM daunorubicin treatment (Figure 4B), and significantly increased resistance at all cytarabine concentrations tested

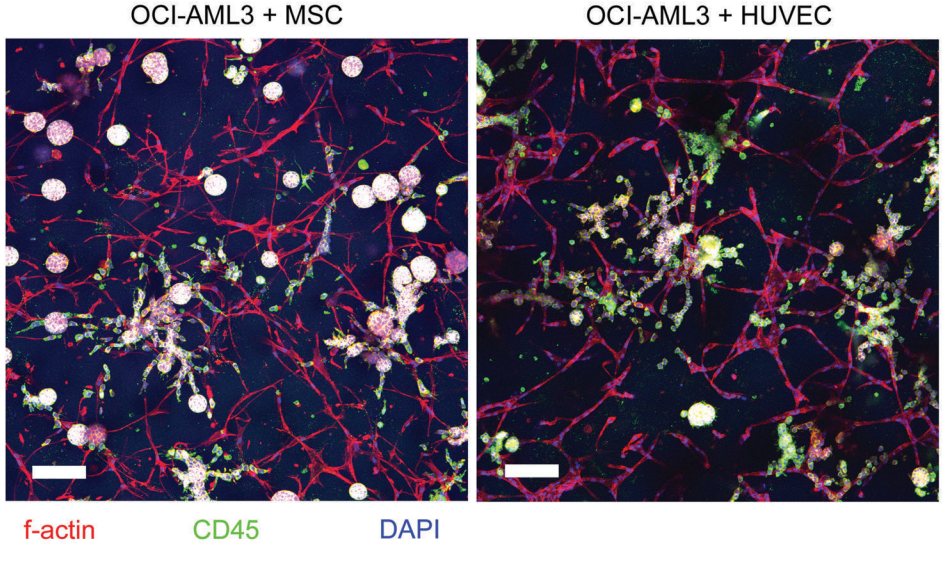

Figure 2. OCI-AML3 co-culture with either human umbilical vein endothelial cells or mesenchymal stem cells. Confocal images of the OCI-AML3 cell line (as a representative of all cell lines utilized in this study) in co-culture with MSC (left) or HUVEC (right) after 7 days of culture. Images display CD45$^+$ leukemia cell growth along both network types. Scale bar = 100 μm.

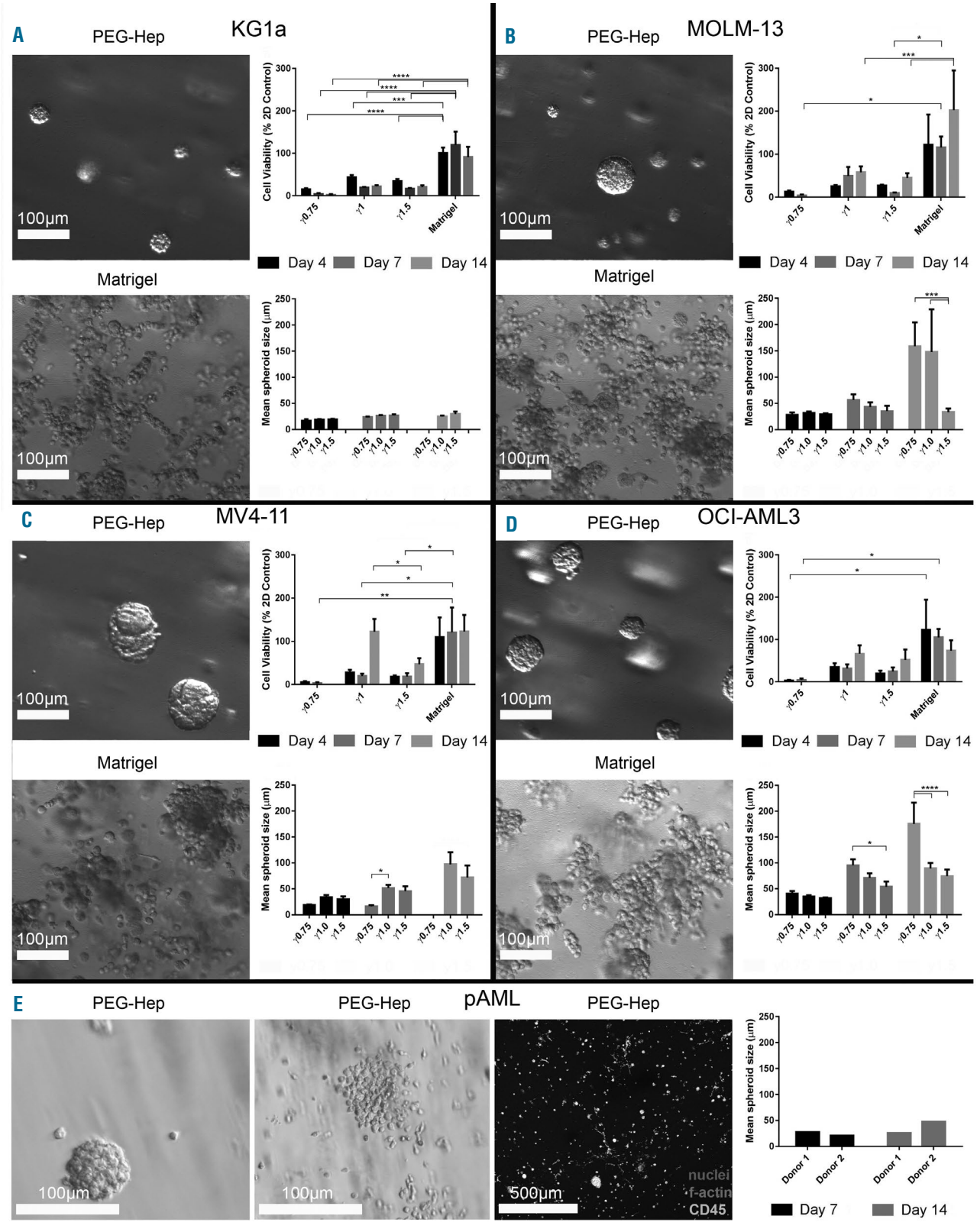

Figure 3. Three-dimensional mono-cultures for the culture of acute myeloid leukemia spheroids. Growth of (A) KG1a, (B) MOLM13, (C) MV4-11 and (D) OCI-AML3 cell lines was investigated in 3D. AML cells were cultured in starPEG-heparin hydrogels (upper left image) or in Matrigel™ (lower left image). Comparison of cell growth (upper right graph) and spheroid size (lower right graph) over 14 days was performed using three different cross-linking degrees of hydrogel (γ0.75, γ1, γ1.5). (E) Primary donor cells from two patients with AML were cultured in starPEG-heparin hydrogels as a mono-culture. Cell line experiments were performed at least twice with three technical replicates (n=2). Data are displayed as mean ± SD. pAML experiments were performed once in triplicate (n=1). The graph displays only the means. Cultures displayed heterogeneous distribution of cells, with each donor's cell growing both as spheroids and single cells. Three photographs per technical replicate were utilized for ImageJ spheroid measurements as a minimum. *Indicates statistical significance: *P<0.05, **P<0.01, ***P<0.001, ****P<0.0001.

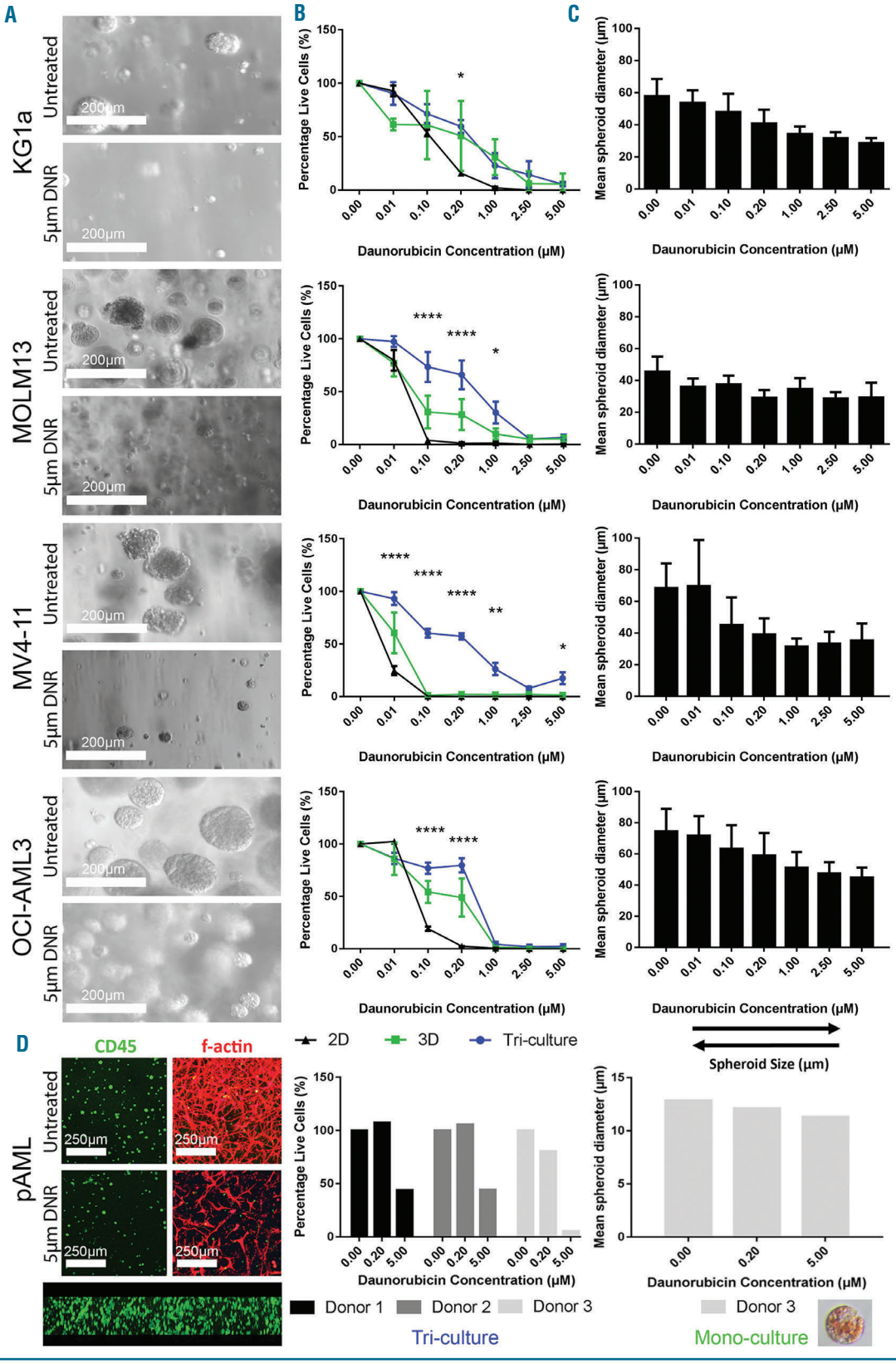

Figure 4. Treatment of three-dimensional mono-cultures and tri-cultures with daunorubicin. (A) Light microscope images of AML cell lines untreated and treated with 5 µM (daunorubicin) DNR at day 7 after treatment. (B) AML cells lines were treated with daunorubicin for 24 h as 2D or 3D mono-cultured, or 3D tri-cultures. Graphs display mean ± SEM. (C) Mean spheroid diameter of 3D mono-cultures after treatment with daunorubicin (± SD). (D) pAML cells from a patient with AML were cultured as 3D mono-cultures (left confocal images) or 3D tri-cultures (right confocal images). Confocal cross-section (bottom confocal image) shows homogeneous distribution of AML mono-culture throughout hydrogel. Mono-cultures (right graph) and tri-cultures (left graph) were treated with two concentrations of daunorubicin. Graphs show only the means. Cell line experiments were performed at least three times in triplicate (n=3-4). pAML experiments were performed once in triplicate (n=1). Three photographs per technical replicate were utilized for ImageJ spheroid measurements as a minimum. Insert in (D) shows daunorubicin uptake into a pAML spheroid (lower right). *Indicates statistical significance between 2D cultures and 3D tri-cultures: *P<0.05, **P<0.01, ***P<0.001, ****P<0.0001.

(*Online Supplementary Figure S4B*). AML spheroid size in mono-cultures was inversely correlated with daunorubicin concentration (Figure 4A,C). Generally, EC_{50} values for tri-cultures were increased in all cell lines when compared with 2D and 3D mono-cultures (Table 1). While pAML cells from donors 1 and 2 only demonstrated reduced viability at 5.00 μM daunorubicin, pAML cells from donor 3 had increased susceptibility to daunorubicin treatment with reduced viability at both 0.20 and 5.00 μM (Figure 4D). Cells from donor 1 demonstrated resistance to cytarabine therapy, while those from donor 2 showed a trend towards decreased viability upon treatment (*Online Supplementary Figure S4D*). The binding constants (Kb) for daunorubicin and cytarabine to the hydrogels reflect the hydrophilic character and number of positively charged groups of the molecules (Table 2). Cytarabine has a higher Kb than daunorubicin, indicating that cytarabine has a slightly higher affinity to the hydrogels (stronger electrostatic interaction with heparin) than daunorubicin. The lower the affinity of a drug to the hydrogels, the easier it is for the drug to diffuse through the hydrogels (*Online Supplementary Figure S7*).

The CXCR4 antagonist, AMD3100, induced mobilization of acute myeloid leukemia cells from the vascular network but failed to increase daunorubicin efficiency in three-dimensional tri-cultures

The CXCR4/CXCR12 axis is thought to be the mechanism through which leukemia cells are protected from chemotherapeutics by the stromal microenvironment.[25-27] Therefore, antagonists targeting this mechanism (e.g. AMD3100) have been developed for use in combination with chemotherapy such as cytarabine or daunorubicin.[28,29] Sorafenib, a multi-tyrosine kinase inhibitor, has also been shown to have antileukemic efficacy when added to standard chemotherapy.[30] The application of AMD3100 significantly reduced AML-vascular contact in KG1a, MOLM13 and MV4-11 cultures (Figure 5A,B). When OCI-AML3 cultures were treated with 2.5 μg/mL AMD3100, a contrasting effect occurred whereby AML-vascular contact increased significantly upon treatment (Figure 5B). Similar results were found for the pAML cultures (Figure 5C). Donors 1 and 3 both displayed decreased AML-vascular contact upon application of AMD3100, while donor 2 showed increased contact (Figure 5C,D). Numbers of viable cells remained unchanged in all three donors after AMD3100 treatment (Figure 5D). Using 3D analysis, no changes in vascular network volume were visualized (*Online Supplementary Figure S8*). However using 2D maximum projection analysis, increased percentage vessel area was found in KG1a and OCI-AML and increased total vessel length was found in OCI-AML3 after AMD3100 treatment (*Online Supplementary Figure S8*). In the pAML cultures, 3D analysis showed increased network volume in donors 1 and 2 and decreased network volume in donor 3 (*Online Supplementary Figure S9*). Using 2D analysis it was seen that donors 1 and 3, but not donor 2, had decreased vessel area and length upon treatment with AMD3100 (*Online Supplementary Figure S9*). CXCR4 expression was similar between MOLM-13, MV4-11 and OCI-AML3 cell lines, whereas some heterogeneity was seen between pAML donors 1 and 2 (*Online Supplementary Figure S10*). When AMD3100 or sorafenib was utilized as a pre-treatment for daunorubicin, no significant increase in daunorubicin toxicity was quantified for all cell lines tested (*Online Supplementary Figure S5A,B*). The binding constants for AMD3100 and sorafenib to the starPEG-heparin hydrogels are presented in Table 2. AMD3100 has a higher Kb than sorafenib, thus indicating that AMD3100 has a higher affinity to the hydrogels whereas the more hydrophobic sorafenib has a low affinity to the hydrogels (*Online Supplementary Figure S7*).

The combination of daunorubicin and cytarabine treatment resulted in complete ablation of acute myeloid leukemia three-dimensional tri-cultures

To mimic the clinical scenario as closely as possible, the approximate values for standard induction therapy, with a combination of cytarabine and daunorubicin, were calculated for traditional human and murine treatments and applied to the 3D cultures based upon the dimensions of the hydrogels (Figure 6A). Five days after treatment, the percentage of live cells was approximately 10% and below (Figure 6B). Tri-cultures were maintained in normal medium for 14 days after treatment to examine any relapse or regrowth of AML cells. However, at day 14 after treatment, cell activity was completely obliterated, or in any case under the detection limit for the cell viability assay. Similar results were observed in the pAML cultures, with all three donors showing few or no metabolically active cells 5 days after treatment (Figure 6C).

Discussion

Vascular endothelial cells are a critical component of the hematopoietic microenvironment that regulates blood cell

Table 1. EC_{50} **half-maximal response values for daunorubicin in KG1a, MOLM13, MV4-11 and OCI-AML3 models.**

Model	Daunorubicin EC_{50} (μM)
KG1a 2D	0.105
KG1a 3D	0.092
KG1a Tri-culture	0.239
MOLM13 2D	0.020
MOLM13 3D	0.038
MOLM13 Tri-culture	0.303
MV4-11 2D	0.006
MV4-11 3D	0.012
MV4-11 Tri-culture	0.178
OCI-AML3 2D	0.057
OCI-AML3 3D	0.132
OCI-AML3 Tri-culture	0.312

Table 2. Observed binding constants of drugs to starPEG-heparin hydrogels.

Drug	Observed binding constant (K_b)
Daunorubicin	$0.87 \pm 0.07\ M^{-1}$
Cytosine β-D-arabinofuranoside (cytarabine)	$3 \pm 0.3\ M^{-1}$
AMD3100	$12.73 \pm 0.17\ M^{-1}$
Sorafenib	$0.79 \pm 0.08\ M^{-1}$

production. The stromal microenvironment promotes malignant progression through signaling factors, cell-matrix and cell-cell interactions or alterations in the surrounding matrix.[31] Although the role of the stromal microenvironment in solid tumor development and progression is well established,[32-34] the role of the stromal niche in AML progression is relatively unknown. Cell-cell interactions between the vascular niche and malignant cell types may play an important role in the pathophysiology of AML. Higher microvascular density is known to occur in the bone marrow microenvironment of patients with hematologic malignancies,[12,35] and may correlate with resistance to therapy.[36] Signaling cross-talk between endothelial and AML cells has been demonstrated in *in vitro* cultures.[37-39] Threfore, AML-vascular niche interactions in AML progression define a pressing area of research.[9]

The growth and capillary network formation of HUVEC within the applied platform of biohybrid glycosaminoglycan hydrogels has previously been demonstrated.[20] Typically, hematopoietic stem cells are found in the vicinity of vascular endothelium.[40] In fact, endothelial cells are

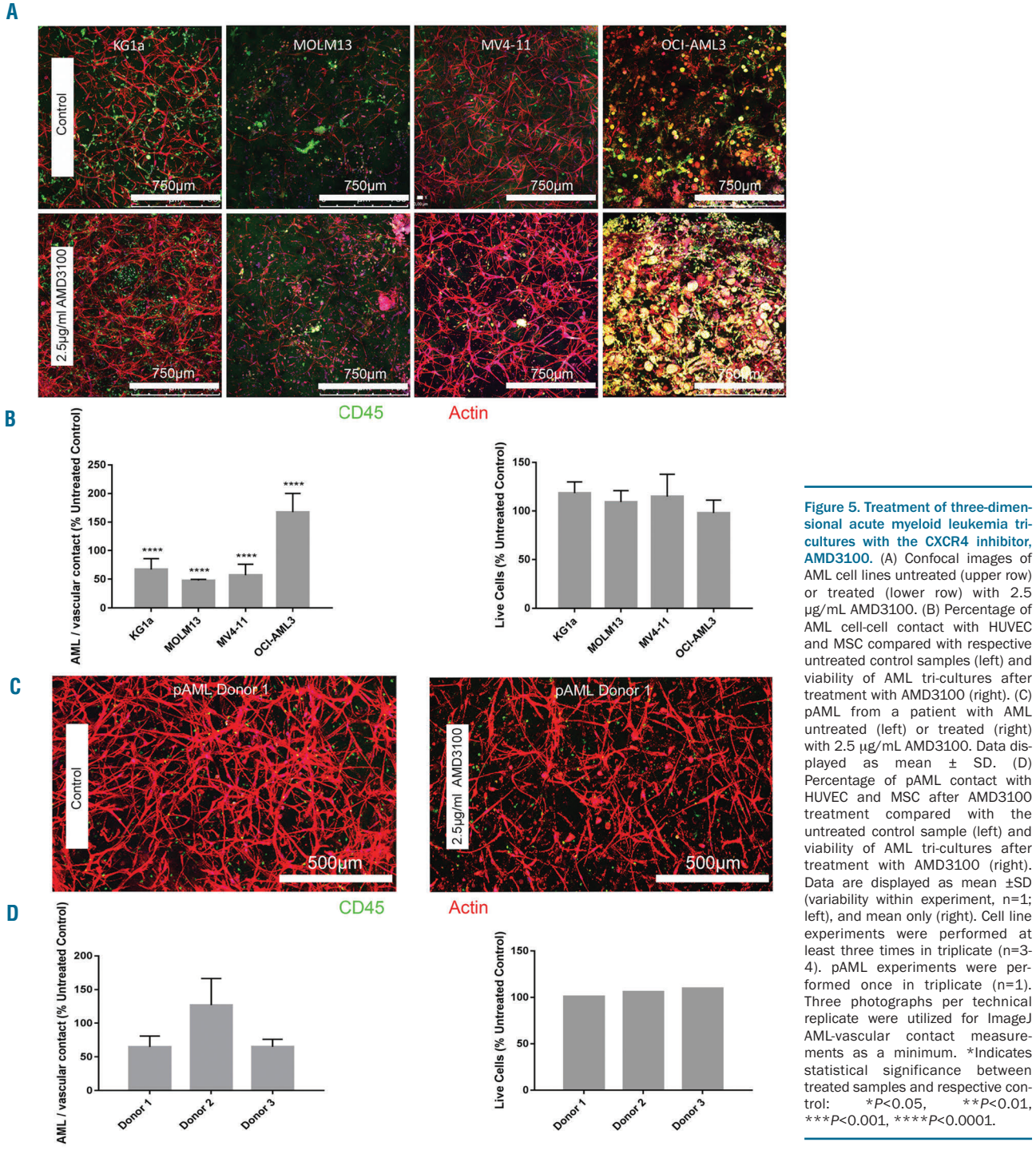

Figure 5. Treatment of three-dimensional acute myeloid leukemia tri-cultures with the CXCR4 inhibitor, AMD3100. (A) Confocal images of AML cell lines untreated (upper row) or treated (lower row) with 2.5 µg/mL AMD3100. (B) Percentage of AML cell-cell contact with HUVEC and MSC compared with respective untreated control samples (left) and viability of AML tri-cultures after treatment with AMD3100 (right). (C) pAML from a patient with AML untreated (left) or treated (right) with 2.5 µg/mL AMD3100. Data displayed as mean ± SD. (D) Percentage of pAML contact with HUVEC and MSC after AMD3100 treatment compared with the untreated control sample (left) and viability of AML tri-cultures after treatment with AMD3100 (right). Data are displayed as mean ±SD (variability within experiment, n=1; left), and mean only (right). Cell line experiments were performed at least three times in triplicate (n=3-4). pAML experiments were performed once in triplicate (n=1). Three photographs per technical replicate were utilized for ImageJ AML-vascular contact measurements as a minimum. *Indicates statistical significance between treated samples and respective control: *P<0.05, **P<0.01, ***P<0.001, ****P<0.0001.

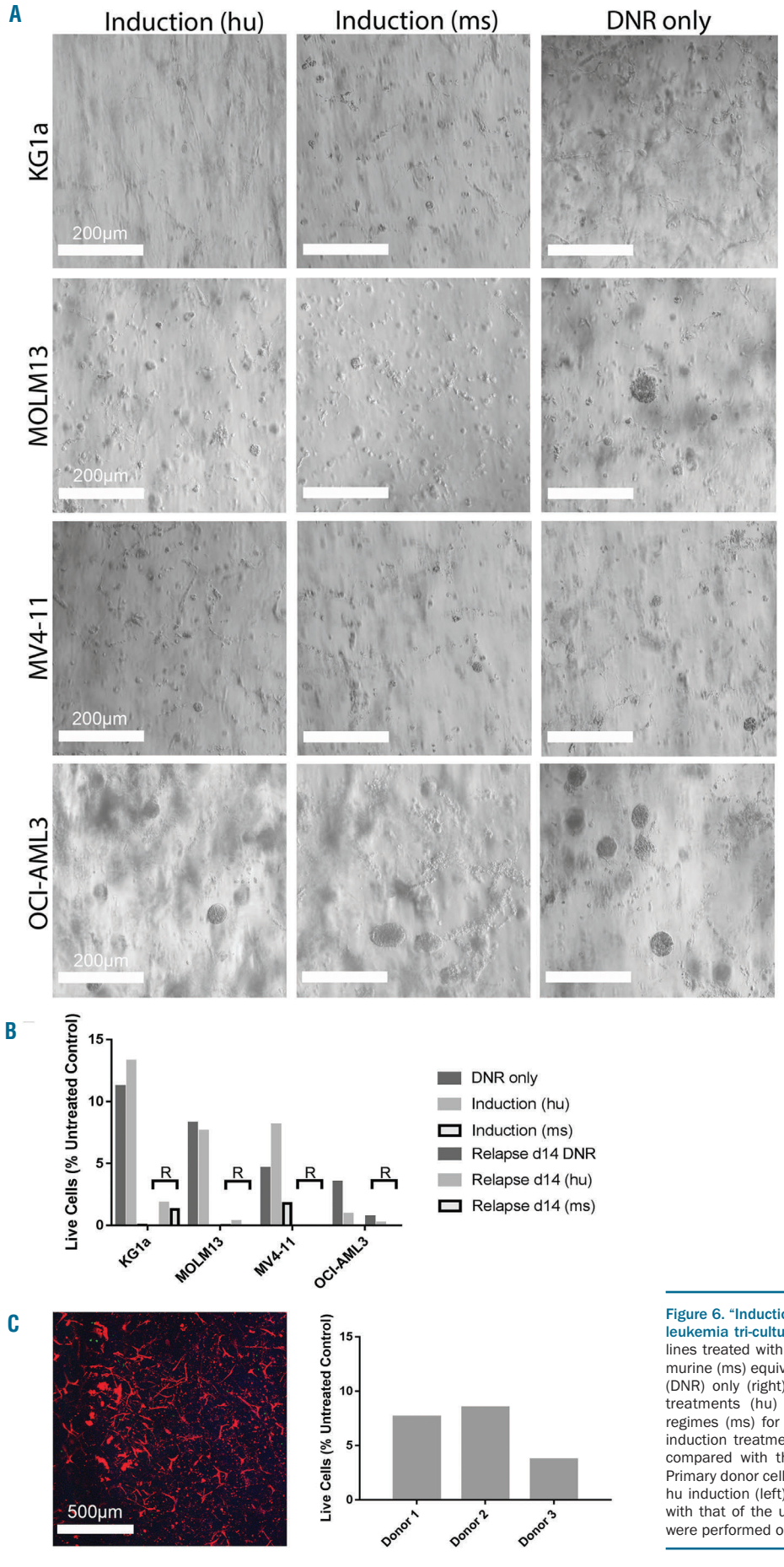

Figure 6. "Induction" treatment and "relapse" of acute myeloid leukemia tri-cultures. (A) Light microscope images of AML cell lines treated with human (hu) equivalent induction dose (left), murine (ms) equivalent induction dose (center) or daunorubicin (DNR) only (right). Doses were based upon standard clinical treatments (hu) or standard murine model chemotherapy regimes (ms) for AML. (B) Percentage of AML live cells after induction treatment and 14 days after treatment (relapse; R) compared with the respective untreated control sample. (C) Primary donor cells (pAML) from a patient with AML treated with hu induction (left). Percentage of pAML cell viability compared with that of the untreated control sample (right). Experiments were performed once in triplicate (n=1).

reported to increase the proliferation of AML cells when in co-culture.[41] AML cells have a reduced cell cycle activity once attached to endothelial cells and are protected from standard chemotherapy. In this context, our results demonstrate the preference for AML cells to adhere to and proliferate on the endothelial network. While pAML cells did not proliferate as fast as the cell lines, they remained in close proximity to the endothelial network. Future studies may explore the role of specific integrins and adhesion molecules in the attachment of AML cells to the vascular endothelium and their localization during 3D mono- and tri-cultures, and integrin inhibition may reveal specific cascades promoting AML-vascular interactions.

In this study, four different AML cell lines were tested to represent various subtypes of AML:[42] KG1a, an M0 classified immature AML cell line, MOLM13, an M5a classified AML cell line known as acute monocytic leukemia, MV4-11, an M5 classified cell line derived from biphenotypic B-myelomonocytic leukemia, and OCI-AML3, an M4 classified AML known as acute myelomonocytic leukemia. In this study, pAML cells derived from three different patients were utilized for the various experiments (*Online Supplementary Table S2*). Donor 1 was a 77-year old male with M2 classified AML (with myelodysplasia-related changes) whose cells were harvested from the bone marrow at initial diagnosis. The AML was negative for *FLT3*-ITD. Donor 2 was a 65-year old male with M1 classified AML (without maturation) whose cells were harvested from the peripheral blood at initial diagnosis. His AML was also negative for *FLT3*-ITD. Donor 3 was a 75-year old male with M1 classified AML (with myelodysplasia-related changes): his cells were harvested from peripheral blood during a progressive/refractory stage of disease. Molecular genetics analysis was not available for this donor due to a lack of molecular testing. With regards to the growth of the four AML cell lines tested, it was seen that the cell viability was reduced in 3D cultures when compared with 2D cultures. AML cells grown within Matrigel™ developed loose clumps of cells, whereas in hydrogels the cells formed tight spheroids. When pAML cells were cultured within our customized biohybrid hydrogels, a heterogeneous population developed, which is typical of an unsorted peripheral blood sample. These results underline the softer mechanical properties and inherent growth factor presence within Matrigel™ in comparison with our glycosaminoglycan-based hydrogels. When cultured to specific time points, the established hydrogel mono-cultures effectively allow the production of AML spheroids of different sizes for subsequent studies.

In our culture model, the AML tri-culture displayed increased resistance at some daunorubicin concentrations using MOLM-13 and MV4-11 cell lines when compared with 2D and 3D mono-cultures, and to a lesser extent in OCI-AML3 cell lines. However, this effect was not visualized in KG1a cultures. Moreover, when cytarabine was applied, our 3D model did not show decreased cell viability, although an increase in treatment concentration or duration of treatment may expose different effects. These findings are similar to those previously reported by other research groups, who suggested that AML cells that are adherent to endothelial cells become more resistant to cytarabine.[17,43] Moreover, cell adhesion-mediated drug resistance to HUVEC and MSC, regulated by integrins, can lead to a decrease in response to chemotherapy.[44] Another important method for the clinical treatment of AML is the use of CXCR4 antagonists to block the CXCR4/CXCL12 axis and prevent AML cells from niche protection, and thus, in theory, make combination therapies more effective. In our hydrogel-based 3D tri-culture model, a significant increase in AML mobilization was observed when AMD3100 was applied to the cultures, except in the case of OCI-AML3. It could be that AMD3100 affects this subtype of AML in an opposing manner, and this method of treatment would not, therefore, be recommended clinically, although, given the high expression of CXCR4 on the surface of OCI-AML3 cells, also associated with poor prognosis,[45,46] it could be that a more potent antagonist is required.[47] It is important to note that differences in HUVEC/MSC network density were sometimes visualized between leukemia cell types in these experiments. It may, therefore, be possible that AMD3100 is in fact altering the network structures, thus making it more difficult for leukemia cells to come into contact with the network, rather than inducing mobilization of leukemia cells. More in-depth 3D quantification is needed to analyze microenvironmental changes in the future and further studies are required to determine the mechanistic effects of AMD3100 on different AML subtypes.

Other than the application of AMD3100, there are several clinically relevant aspects of our study. Induction treatment is given to AML patients as a 'first-line' therapy. Usually, induction therapy results in ablation of the bulk of malignant cells in order to remove the leukemia from the patients' hematopoietic system. To eradicate the residual leukemic cells, further consolidation therapy is applied, ideally to extinguish even minimal residual disease and to achieve a cure. Our data here show the effectiveness of equivalent induction therapy doses on our 3D microenvironment model, and complete ablation of leukemia cell lines without re-growth after 2 weeks. Future experiments should explore the development of long-term cultures (3-6 months) and the effects of induction therapy, relapse and consolidation therapy. As the minimal residual disease status after chemotherapy is of major prognostic significance,[48] the biology and dynamics of residual leukemia cells after therapy could be an interesting application of the novel tri-culture model.

Using specimens from AML patients as well as cell lines, we provide experimental evidence supporting the clinical relevance of our results. We have demonstrated not only that AML interactions with vascular endothelial cells are modulated by the CXCR4/CXCL12 axis within our engineered microenvironments, but also that not all subtypes of AML respond in the same way. We must also state the limitations of the study here, in which pAML experiments were performed with three patients' samples in parallel triplicates; the conclusions drawn from our studies should, therefore, be considered exploratory. Although detailed risk classifications, based mainly on genetic abnormalities, have been shown to project the outcome of patient cohorts accurately, the outcome of individual patients still remains quite unpredictable. Additional information, for example on responsiveness towards a treatment approach, would therefore provide a new perspective to refine outcome predictions. Standard treatments are recommended for AML patients because of known improved outcomes, however with the absence of a personalized testing system, patients who do not respond to standard treatments

are left without targeted disease management. Hence, our findings provide a new perspective on the impact of drug treatments, both standard and those in trials, on cell-cell interactions in a 3D microenvironment.

In summary, our AML tri-culture model enables extensive analysis of leukemia-vascular interactions. Relying on a thoroughly tunable hydrogel matrix platform, AML cells have been, for the first time, successfully co-cultured with both HUVEC and MSC. Importantly, the approach offers exciting, unprecedented options for the visualization of AML-vascular interactions after the application of anti-cancer compounds, which is particularly important for investigating the impact of chemotherapeutics on post-application cellular responses. The response of our model to the administration of anti-CXCR4 demonstrated mobilization of leukemia cells from the vascular niche, supporting the *in vivo*-like behavior of the organotypic scaffold. Moreover, our 3D AML co-cultures showed a significantly increased resistance to chemotherapeutics compared with 2D cultures, confirming the greater clinical relevance of the hydrogel-based model we presented. We anticipate that the approach will become instrumental in future extensive chemotherapeutic-signaling inhibitor combination treatment analyses as well as in the definition of individualized treatment modalities for AML patients. Beyond that, identification of the signaling mechanisms of endothelial cells within the vascular niche which encourage AML growth or provide resistance to conventional chemotherapy might provide new insights for the development of novel therapeutic strategies for AML patients.

Acknowledgments

LJB was supported by the Endeavour Awards as part of the Prime Minister's Australia Awards. Financial support was provided by the German Research Foundation (Deutsche Forschungsgemeinschaft) through grant numbers: SFB-TR 67, WE 2539-7 and FOR/EXC999, by the Leibniz Association (SAW-2011-IPF-2 68) and by the European Union through the Integrated Project ANGIOSCAFF (Seventh Framework Program). The authors gratefully thank Dr Manja Wobus, Dr Mikhail Tsurkan, Mrs Juliane Drichel, Mrs. Milauscha Grimmer and Mr Christoph Hentschel for their advice and assistance.

References

1. Appelbaum FR, Rowe JM, Radich J, Dick JE. Acute myeloid leukemia. Hematology Am Soc Hematol Educ Program. 2001;62-86.
2. NCI Network. Trends in incidence and outcome for haematological cancers in England: 2001-2010. London: Public Health England, 2014.
3. Visser O, Trama A, Maynadie M, et al. Incidence, survival and prevalence of myeloid malignancies in Europe. Eur J Cancer. 2012;48(17):3257-3266.
4. Pickup MW, Mouw JK, Weaver VM. The extracellular matrix modulates the hallmarks of cancer. EMBO Rep. 2014;15(12):1243-1253.
5. Radisky D, Muschler J, Bissell MJ. Order and disorder: the role of extracellular matrix in epithelial cancer. Cancer Invest. 2002;20(1):139-153.
6. Aljitawi OS, Li D, Xiao Y, et al. A novel three-dimensional stromal-based model for in vitro chemotherapy sensitivity testing of leukemia cells. Leuk Lymphoma. 2014;55(2):378-391.
7. Blanco TM, Mantalaris A, Bismarck A, Panoskaltsis N. The development of a three-dimensional scaffold for ex vivo biomimicry of human acute myeloid leukaemia. Biomaterials. 2010;31(8):2243-2251.
8. Velliou EG, Dos Santos SB, Papathanasiou MM, et al. Towards unravelling the kinetics of an acute myeloid leukaemia model system under oxidative and starvation stress: a comparison between two- and three-dimensional cultures. Bioprocess Biosyst Eng. 2015;38(8):1589-1600.
9. Trujillo A, McGee C, Cogle CR. Angiogenesis in acute myeloid leukemia and opportunities for novel therapies. J Oncol. 2012;2012:128608.
10. Kopp HG, Avecilla ST, Hooper AT, Rafii S. The bone marrow vascular niche: home of HSC differentiation and mobilization. Physiology (Bethesda). 2005;20:349-356.
11. Dias S, Hattori K, Heissig B, et al. Inhibition of both paracrine and autocrine VEGF/VEGFR-2 signaling pathways is essential to induce long-term remission of xenotransplanted human leukemias. Proc Natl Acad Sci USA. 2001;98(19):10857-10862.
12. Hussong JW, Rodgers GM, Shami PJ. Evidence of increased angiogenesis in patients with acute myeloid leukemia. Blood. 2000;95(1):309-313.
13. Padro T, Ruiz S, Bieker R, et al. Increased angiogenesis in the bone marrow of patients with acute myeloid leukemia. Blood. 2000;95(8):2637-2644.
14. Butler JM, Kobayashi H, Rafii S. Instructive role of the vascular niche in promoting tumour growth and tissue repair by angiocrine factors. Nature Rev Cancer. 2010;10(2):138-146.
15. Doan PL, Chute JP. The vascular niche: home for normal and malignant hematopoietic stem cells. Leukemia. 2012;26(1):54-62.
16. Ribatti D. Bone marrow vascular niche and the control of tumor growth in hematological malignancies. Leukemia. 2010;24(7):1247-1248.
17. Pezeshkian B, Donnelly C, Tamburo K, Geddes T, Madlambayan GJ. Leukemia mediated endothelial cell activation modulates leukemia cell susceptibility to chemotherapy through a positive feedback loop mechanism. PLoS One. 2013;8(4):e60823.
18. Freudenberg U, Hermann A, Welzel PB, et al. A star-PEG-heparin hydrogel platform to aid cell replacement therapies for neurodegenerative diseases. Biomaterials. 2009;30(28):5049-5060.
19. Tsurkan MV, Chwalek K, Prokoph S, et al. Defined polymer-peptide conjugates to form cell-instructive starPEG-heparin matrices in situ. Adv Mater. 2013;25(18):2606-2610.
20. Chwalek K, Tsurkan MV, Freudenberg U, Werner C. Glycosaminoglycan-based hydrogels to modulate heterocellular communication in in vitro angiogenesis models. Sci Rep. 2014;4:4414.
21. von Bonin M, Wermke M, Cosgun KN, et al. In vivo expansion of co-transplanted T cells impacts on tumor re-initiating activity of human acute myeloid leukemia in NSG mice. PLoS One. 2013;8(4):e60680.
22. Chwalek K, Levental KR, Tsurkan MV, Zieris A, Freudenberg U, Werner C. Two-tier hydrogel degradation to boost endothelial cell morphogenesis. Biomaterials. 2011;32(36):9649-9657.
23. Oswald J, Boxberger S, Jorgensen B, et al. Mesenchymal stem cells can be differentiated into endothelial cells in vitro. Stem Cells. 2004;22(3):377-384.
24. Bray LJ, Binner M, Holzheu A, et al. Multi-parametric hydrogels support 3D in vitro bioengineered microenvironment models of tumour angiogenesis. Biomaterials. 2015;53:609-620.
25. Burger JA, Kipps TJ. CXCR4: a key receptor in the crosstalk between tumor cells and their microenvironment. Blood. 2006;107(5):1761-1767.
26. Burger JA, Tsukada N, Burger M, Zvaifler NJ, Dell'Aquila M, Kipps TJ. Blood-derived nurse-like cells protect chronic lymphocytic leukemia B cells from spontaneous apoptosis through stromal cell-derived factor-1. Blood. 2000;96(8):2655-2663.
27. Tavor S, Petit I. Can inhibition of the SDF-1/CXCR4 axis eradicate acute leukemia? Semin Cancer Biol. 2010;20(3):178-185.
28. Burger JA, Peled A. CXCR4 antagonists: targeting the microenvironment in leukemia and other cancers. Leukemia. 2009;23(1):43-52.
29. Juarez J, Bradstock KF, Gottlieb DJ, Bendall LJ. Effects of inhibitors of the chemokine receptor CXCR4 on acute lymphoblastic leukemia cells in vitro. Leukemia. 2003;17(7):1294-1300.
30. Rollig C, Serve H, Huttmann A, et al. Addition of sorafenib versus placebo to standard therapy in patients aged 60 years or younger with newly diagnosed acute myeloid leukaemia (SORAML): a multicentre, phase 2, randomised controlled trial.

Lancet Oncol. 2015;16(16):1691-1699.
31. Micke P, Ostman A. Tumour-stroma interaction: cancer-associated fibroblasts as novel targets in anti-cancer therapy? Lung Cancer. 2004;45 (Suppl 2):S163-175.
32. Dvorak HF, Weaver VM, Tlsty TD, Bergers G. Tumor microenvironment and progression. J Surg Oncol. 2011;103(6):468-474.
33. Hanahan D, Coussens LM. Accessories to the crime: functions of cells recruited to the tumor microenvironment. Cancer Cell. 2012;21(3):309-322.
34. Lathia JD, Heddleston JM, Venere M, Rich JN. Deadly teamwork: neural cancer stem cells and the tumor microenvironment. Cell Stem Cell. 2011;8(5):482-485.
35. Ribatti D. Is angiogenesis essential for the progression of hematological malignancies or is it an epiphenomenon? Leukemia. 2009;23(3):433-434.
36. Ayala F, Dewar R, Kieran M, Kalluri R. Contribution of bone microenvironment to leukemogenesis and leukemia progression. Leukemia. 2009;23(12):2233-2241.
37. Hatfield K, Oyan AM, Ersvaer E, et al. Primary human acute myeloid leukaemia cells increase the proliferation of microvascular endothelial cells through the release of soluble mediators. Br J Haematol. 2009;144(1):53-68.
38. Hatfield KJ, Evensen L, Reikvam H, Lorens JB, Bruserud O. Soluble mediators released by acute myeloid leukemia cells increase capillary-like networks. Eur J Haematol. 2012;89(6):478-490.
39. Liesveld JL, Rosell KE, Lu C, et al. Acute myelogenous leukemia--microenvironment interactions: role of endothelial cells and proteasome inhibition. Hematology. 2005;10(6):483-494.
40. Kiel MJ, Yilmaz OH, Iwashita T, Yilmaz OH, Terhorst C, Morrison SJ. SLAM family receptors distinguish hematopoietic stem and progenitor cells and reveal endothelial niches for stem cells. Cell. 2005;121(7): 1109-1121.
41. Hatfield K, Ryningen A, Corbascio M, Bruserud O. Microvascular endothelial cells increase proliferation and inhibit apoptosis of native human acute myelogenous leukemia blasts. Int J Cancer. 2006;119 (10):2313-2321.
42. Bennett JM, Catovsky D, Daniel MT, et al. Proposals for the classification of the acute leukaemias. French-American-British (FAB) co-operative group. Br J Haematol. 1976;33(4):451-458.
43. Cogle CR, Goldman DC, Madlambayan GJ, et al. Functional integration of acute myeloid leukemia into the vascular niche. Leukemia. 2014;28(10):1978-1987.
44. Damiano JS, Cress AE, Hazlehurst LA, Shtil AA, Dalton WS. Cell adhesion mediated drug resistance (CAM-DR): role of integrins and resistance to apoptosis in human myeloma cell lines. Blood. 1999;93(5):1658-1667.
45. Konoplev S, Rassidakis GZ, Estey E, et al. Overexpression of CXCR4 predicts adverse overall and event-free survival in patients with unmutated FLT3 acute myeloid leukemia with normal karyotype. Cancer. 2007;109(6):1152-1156.
46. Rombouts EJ, Pavic B, Lowenberg B, Ploemacher RE. Relation between CXCR-4 expression, Flt3 mutations, and unfavorable prognosis of adult acute myeloid leukemia. Blood. 2004;104(2):550-557.
47. Cho BS, Zeng Z, Mu H, et al. Antileukemia activity of the novel peptidic CXCR4 antagonist LY2510924 as monotherapy and in combination with chemotherapy. Blood. 2015;126(2):222-232.
48. Shayegi N, Kramer M, Bornhauser M, et al. The level of residual disease based on mutant NPM1 is an independent prognostic factor for relapse and survival in AML. Blood. 2013;122(1):83-92.